UNIVERSIDADE DE SÃO PAULO

INSTITUTO DE FÍSICA
CAIXA POSTAL 20516
01498 SÃO PAULO - SP
BRASIL

PUBLICAÇÕES

IFUSP/P-938

TRAJECTORIES OF QUASI-INTEGRABLE FIELD LINES IN TOKAMAKS

M.C. Ramos de Andrade, I.L. Caldas and **M.V.A.P. Heller**
Instituto de Física, Universidade de São Paulo

Setembro/1991

TRAJECTORIES OF QUASI-INTEGRABLE FIELD LINES IN TOKAMAKS[+]

M. C. Ramos de Andrade[*], I. L. Caldas, M. V. A. P. Heller

Instituto de Fisica da Universidade de São Paulo ,

C.P. 20516, 01498 - São Paulo-SP, Brazil

Abstract: A method to describe the behaviour of a quasi-integrable system composed by an equilibrium plasma in a tokamak perturbed by resonant helical fields is presented. The perturbative method, which takes into account the toroidal correction introduced to the system, modifies the Hamiltonian equations in action-angle variables (J,ϑ), obtained to describe the initial integrable field, and provides approximate differential equations that describe the trajectories of the magnetic field lines of the quasi-integrable system in the plane (J,ϑ). The Poincaré maps, obtained from the integration of the exact equations of the magnetic field lines are compared with those obtained from the integration of the equations resulted from the perturbative method and the validity of the method is analysed.

+This work is partially supported by FAPESP, CNPq and FINEP.

*Present Address: JET Joint Undertaking, Abingdon, Oxon-OX14 3EA, UK.

I - INTRODUCTION

The plasma confinement in tokamaks depends upon the existence of toroidal magnetic surfaces. These surfaces are present in the system when there is some spatial symmetry in the magnetic field configuration[1]. However, they can be partially destroyed by resonant helical perturbations due to plasma oscillations[2] or external currents [3]. Experiments with external helical windings have shown that plasma confinement can be controlled and the disruptive instability can be investigated[2,3,4]. Besides this, the disruptive instability seems to be related with the destruction of the magnetic surfaces due to the overlapping of magnetic islands generated by these helical resonances[5,6].

Starting from an axi-symmetric plasma in MHD equilibrium confined in a large aspect-ratio tokamak and perturbed by a field produced by external helical currents I_h, we establish, in section II, exact equations for the field lines and a Hamiltonian formalism described in action-angle variables (J,ϑ). This is possible because the perturbed system with helical symmetry is integrable. The helical perturbation changes the magnetic field configuration and leads to the appearance of magnetic islands around the resonant surface.

The introduction of the toroidal correction to this configuration causes the break-up of symmetry of the system as well as of its integrability [7,8]. Besides this, the secondary islands which appear due to the introduction of the toroidal effect can overlap with the primary islands that already existed in the system leading to the

destruction of magnetic surfaces. In order to describe the non-integrable field we use, in section III, a perturbation method to obtain approximate differential equations which are numerically integrated and supply the Poincaré map of the field lines. This map characterizes the distribution of magnetic surfaces in the system and the structure of primary and secondary islands as well as the appearance of a chaotic region due to the destruction of magnetic surfaces. In section III the expansion of the chaotic region between resonant surfaces can be analysed in terms of the increase of the helical currents and the decrease of the tokamak aspect-ratio.

In this paper we compare the results obtained from the numerical integration of the equations that are deduced from the perturbative method with those provided by the numerical integration of the exact magnetic field lines. In this way, we are able to evaluate the conditions under which the perturbative theory is valid in order to have further applications in the study of quasi-integrable Hamiltonian systems as we point out through this paper. The Hamiltonian formalism presented here describes a system in a large aspect-ratio tokamak and can be employed for other toroidal machines like a stellarator[9] or a levitron[10].

II - HAMILTONIAN FORMULATION TO THE MAGNETIC FIELD LINES

Let us consider an axi-symmetric plasma in static MHD equilibrium confined in a large aspect-ratio tokamak (R/a >>1, where R and a are respectively the major and minor plasma radii) which is

described in a cylindrical geometry with periodicity $2\pi R$. The equilibrium field is given by the sum of a uniform toroidal field B_z^0 and a poloidal field B_θ^0 produced by the plasma current density given by:

$$\mathbf{J} = \frac{I_p\,(\gamma+1)}{\pi\, a^2}\left(1 + \frac{r^2}{a^2}\right)^{\gamma} \hat{e}_z \qquad (1)$$

where I_p is the plasma current and γ is a constant parameter. For this equilibrium the magnetic surfaces establish a system of nested concentric cylinders and the safety factor is given by:

$$q(r) = \frac{r\, B_z^0}{R\, B_\theta^0} \qquad (2)$$

The equilibrium plasma is perturbed by a helical field B_1 produced by m pairs of adjacent and equidistant conductors in the form of a cylindrical spiral of radius b in which the currents I_h flow in opposite directions (fig.1). This field has helical symmetry and the resulting system is considered to be described by the superposition of the unperturbed field with the perturbation B_1 as follows:

$$\mathbf{B} \simeq \mathbf{B}^0(r) + \mathbf{B}_1(r,u) \qquad (3)$$

In (3) $B_1/B^0 \ll 1$ and $u = m\theta - kz$ where $k = n/R$ is the modulus of the z component of the wave vector and m and n are integer numbers that determine the helicity of the field through the ratio m/n. The approximation (3) is allowed when marginally stable states are not

present in the system.

From the equations for magnetic field lines:

$$\frac{dr}{B_r} = \frac{r\,d\theta}{B_\theta} = \frac{dz}{B_z} \qquad (4)$$

and taking into account that $B_1 = \nabla\phi$, where ϕ is the scalar potential given by:[8]

$$\phi \simeq \frac{2\,\mu_0\,b\,I_h\,k}{\pi} K'_m(kb)\, I_m(kr)\, \mathrm{sen}\,u \qquad (5)$$

we can write from (3), (4) and (5):

$$B_z \frac{dr}{dz} = \frac{2\,\mu_0\,b\,I_h\,k^2}{\pi} K'_m(kb) I'_m(kr) \mathrm{sen}\,u \qquad (6.a)$$

$$B_z \frac{du}{dz} = \frac{m\,B_\theta^0}{r} - kB_z^0 + \frac{2\,\mu_0\,b\,I_h\,k^3}{\pi} K'_m(kb) I_m(kr)\,\cos u \left(\frac{m^2}{r^2k^2}+1\right) \qquad (6.b)$$

where I_m and K_m are the modified Bessel functions of first and second types respectively[1] and the derivatives are taken with respect to the argument (kr).

The equations (6) can be written in a Hamiltonian

form as follows,

$$\frac{\partial \mathcal{H}}{\partial \rho} = -\frac{du}{dt} \qquad (7.a) \qquad \frac{\partial \mathcal{H}}{\partial u} = \frac{d\rho}{dt} \qquad (7.b)$$

since we introduce the variables:

$$B_z = \frac{dz}{dt} \qquad (8)$$

and

$$\rho = \frac{1}{2} r^2 \qquad (9)$$

In eqs. (7) the Hamiltonian $\mathcal{H}$ given by:

$$\mathcal{H} = \frac{k\,B_z^0\,r^2}{2} - m\int^r B_\theta^0(r')\,dr' + \frac{\mu_0\,I_h\,m}{\pi}\left(\frac{r}{b}\right)^m \cos u \qquad (10)$$

is invariant along the field lines and, consequently, represents the magnetic surfaces for the system. In (10) we have expanded the Bessel functions in the limit where their arguments tend to zero since we are interested in the region where $kb \ll 1$, $kr \ll 1$ and $r < b$.

The orbit equations in the (ρ,u) plane are defined by the equation:

$$\frac{d\rho}{du} = \frac{d\rho/dt}{du/dt} = \frac{-\partial\mathcal{H}/\partial u}{\partial\mathcal{H}/\partial\rho} \qquad (11)$$

and the intersections of the magnetic surfaces with a plane $t = c^{te}$ can be obtained from the numerical integration of equation (11)[13].

Since the system previously described is integrable we define, through a canonical tranformation, action-angle variables (J,ϑ) that provide field line equations which are easily integrated. Standard procedures lead us to[11]:

$$J = J(\mathcal{H}) = \frac{1}{4\pi}\oint r^2\,du \qquad (12) \qquad \omega = \omega(J) = \frac{d\mathcal{H}(J)}{dJ} \qquad (13)$$

and the field line equations become:

$$\frac{dJ}{dt} = 0 \qquad (14.a) \qquad\qquad \frac{d\vartheta}{dt} = \omega(J) \qquad (14.b)$$

with the variable ϑ given by:

$$\vartheta = \frac{\partial S(u,J)}{\partial J} \qquad (15)$$

and the generating function S defined by:

$$S(u,J) = \frac{1}{2}\int_{u_0}^{u} r^2\,du \qquad (16)$$

with u_0 constant.

The frequency $\omega(J)$ can be related to the frequency of field lines rotation $\omega_0 = \delta\theta/\delta z$ through the equation[13]:

$$\omega = \frac{d\vartheta}{dt} = \frac{\delta\vartheta}{\delta u}\frac{\delta u}{\delta z}\frac{dz}{dt} = (k - \omega_0 m)\,B_z = \left(kB_z - m\frac{B_\theta}{r}\right) \qquad (17)$$

where we have used the eq.(4). The expression (17) provides an accurate estimation of the values of $\omega(J)$ as we can see by comparing the curves in the fig.2.

III - THE TOROIDAL EFFECT AND THE PERTURBATIVE METHOD

In this section we analyse what occurs in the system when the correction associated with the curvature of the magnetic field lines in a torus is introduced.

In this case the equations (14) are not valid any more because the integrability of the system is broken due to the lack of symmetry resulting in the destruction of the magnetic surfaces[1]. However, for a small helical perturbation, the strongest effect on a large aspect-ratio tokamak, due to the introduction of the toroidal effect, is the appearance of $(m \pm 1)$ satellite magnetic islands on the rational magnetic surfaces with $q = m \pm 1$ [12] (fig.3). The overlapping of primary and secondary islands may lead to the destruction of magnetic surfaces and consequently to the appearance of a chaotic region in the plasma whose extension depends on the ratio

a/R and on the amplitude of the helical currents I_h.

The toroidal correction is considered by multiplying the constant field B_z^0, in the field line equations (4), by the factor $[\,1 - \varepsilon\cos\theta\,]^{-1}$. These equations are expanded and the leading terms in ε ($\varepsilon = -r/R$) are retained. From the resulting equations we identify an expression for the magnetic field as given by[13,15]:

$$B = B_0(r) + \nabla\phi + \varepsilon\cos\theta\,\nabla\phi \qquad (18)$$

Taking into account eqs.(4) and (8) we have for the field line equations, corrected up to first order in ε,

$$\frac{dr}{dt} = B_r = \frac{dr_0}{dt} + \varepsilon\cos\theta\,\frac{dr_1}{dt} \qquad (19.a)$$

$$\frac{du}{dt} = m\,\frac{B_\theta}{r} - kB_z = \frac{du_0}{dt} + \varepsilon\cos\theta\,\frac{du_1}{dt} \qquad (19.b)$$

where the zero index refers to the integrable field and the "1" index refers to the toroidal correction introduced to the system. The equations in the (J,θ) variables can be written as follows:

$$\frac{dJ}{dt} = \frac{dJ}{d\mathcal{H}}\left[\frac{\partial\mathcal{H}}{\partial r_0}\frac{dr}{dt} + \frac{\partial\mathcal{H}}{\partial u_0}\frac{du}{dt}\right] \qquad (20.a)$$

$$\frac{d\theta}{dt} = \frac{d\theta_0}{dt}\,\frac{du}{dt} = \frac{d\theta_0/dt}{du_0/dt}\,\frac{du}{dt} \qquad (20.b)$$

From eqs.(7), (14.b), (18), (19) and (20) we have[13]:

$$\frac{dJ}{dt} = \frac{\varepsilon r\cos\theta}{\omega}\left(kB_z^0 - \frac{m}{r}B_\theta^0(r)\right)\frac{\partial\phi}{\partial r} \qquad (21.a)$$

$$\frac{d\theta}{dt} = \omega + \frac{\varepsilon\omega\cos\theta\left(\frac{m}{r^2}\,\frac{\partial\phi}{\partial\theta}\right)}{-kB_z^0 + \frac{m}{r}\left[B_\theta^0 + \frac{1}{r}\,\frac{\partial\phi}{\partial\theta}\right]} \qquad (21.b)$$

where ϕ is given by equation (5) and we have considered terms up to the order of ε.

We may notice from eqs.(21) that when either $\varepsilon \mapsto 0$ or $I_h \mapsto 0$ ($\phi \mapsto 0$), the integrable equations are recovered. The maps of the field line trajectories in the (J,θ) plane obtained by integrating the eqs.(21) can be seen in fig.4.

Moreover, we can check the validity of the method by carrying out the numerical integration of the exact field line equations and comparing both results as described in the next section.

IV - NUMERICAL RESULTS

The map of the magnetic field lines in the plane (J,ϑ), obtained by integrating eq.(21) can be compared with the one obtained from the integration of the exact field line equations (4) which are corrected by the toroidal effect (i.e., by multiplying B_z^0 by $[1 - \varepsilon\cos\theta]^{-1}$). This integration consists of taking an initial pair of coordinates (ρ_0, u_0) and integrating the field line equations along several toroidal turns. Each pair of coordinates (ρ,u), obtained after each turn, is transformed into the pair of action-angle variables (J,ϑ) by using equations (12), (15) and (16). These points (J,ϑ) are collected and the map of the field lines can be constructed (fig.5). All the calculations were made with the parameters of the tokamak TBR-1: a=8cm, R=30cm and b=11cm (fig.1). The typical plasma current is I_p=10kA and the current in the helical windings is I_h=100A. The results obtained from the integration of eqs.(21) show that, for points (ρ,u) positioned outside of the resonant region, the corresponding action J is approximately constant as in the case r = 5.8cm and u = 0 (fig.4). This is so because in this region the system behaves itself as if it was integrable and following approximately the eqs.(14). On the other hand, for initial points (ρ_0, u_0) placed around the resonant surface and taken where the magnetic surfaces start being destroyed, we can observe chaotic behaviour of the J values as its shown on fig.4 where the map $J \times \vartheta$ shows the behaviour of field lines with starting points $u_0 = \pi/2$ and r_0 = 5.8 and 6.4cm. The primary islands are around the surface with q = 3 which corresponds to a radius of 6.2cm. Still regarding fig.4

and looking at the initial point at the radius close to the surface with q = 2, ($r_{2,1} \simeq 4.7$cm) we can observe periodic structures which are related to the satellite islands present around these surface. All the figures were obtained for q(a) = 5, q(0) = 1, I_p = 10kA, I_h = 100A, m = 3 and n = 1. The frequency ω, defined in eq.(13), can be obtained as a function of ρ by considering two distinct methods. One of them corresponds to the numerical integration of eq.(13) itself and the second one consists of calculating ω by taking eq.(17). The fig. 2 shows the two plots obtained and the comparison of the two results allows us to estimate quite well the value of ω by equation (17).

By comparing the (J,ϑ) maps which result from the integration of the exact field lines and from the perturbative method (figs.5 and 4 respectively) we can say that the behaviour of the field lines can be predicted somehow by the equations described by the perturbative method. Not only the values of action but the field lines behaviour itself can be reasonably estimated. Moreover, the region where the magnetic surfaces start being destroyed can be observed as well. The non closed periodic structures which appear at fig. 4 around the radius r=4.7cm can be explained by the fact that the perturbative method is valid up to a certain number of toroidal turns after which it does not reproduce the (J,ϑ) points obtained by integrating the exact field equation. Anyway it seems that the method is a powerfull tool to be used in the study of quasi-integrable Hamiltonian systems.

V - SUMMARY AND CONCLUSIONS

In this paper we estimate the behaviour of the magnetic surfaces in a large aspect-ratio tokamak when the toroidal correction is taken upon an integrable system consisted by an axi-symmetric plasma in a static equilibrium MHD, perturbed by the field generated by three pairs of equidistant helical conductors, which are placed along the torus (the helical current I_h flows the adjacent windings in opposite directions).

In order to carry on with this analysis we initially described the evolution of the magnetic field lines through a Hamiltonian formulation where we introduced action-angle variables (J,ϑ) since the system was integrable. The equations that follow from this formalism are altered when the toroidal correction is taken into account since the integrability of the system is broken. The non integrable field is then described by a perturbation method which provides approximate differential equations that, when numerically integrated, supply the map of Poincaré of the field lines.

When we compare the results of the integration of the exact field lines with those related to the integration of the equations resulted from the perturbative method, we see that this method provides a good estimation of the behaviour of the magnetic field lines as long as it confirms the quasi-integrable nature of the system by characterizing the region for which the action variable J remains approximately constant and the regions where it becomes chaotic due to the break up of the magnetic surfaces of the system. Besides this, the method predicts the appearance of the satellite

islands around the surfaces with $q = m \pm 1$ even though we obtain meaningfull results up to a certain number of toroidal turns after which the method seems not to predict the field behaviour very well. In spite of this, the method seems to be a good tool to study quasi-integrable Hamiltonian systems and, as a next step, it might be possible to write the equations (21) in a Hamiltonian form, even if the Hamiltonian formulation to describe quasi-integrable two degrees of freedom systems is not trivial, in order to apply the renormalization theory, proposed by Escande, where the condition for the destruction of the last magnetic surface between two resonances is analysed by looking at an expanded region of the phase space between these resonances and taking into account the tendency of their amplitudes at each step of the renormalization process[14].

ACKNOWLEDGEMENTS - The authors would like to thank W. P. de Sá (São Paulo University) for useful suggestions regarding the numerical calculations.

VI - REFERENCES

1 - MOROZOV A. I., SOLOV'EV L. S. - Reviews of Plasma Physics 2, Consultants Bureau, New York (1966).

2 - ROBINSON D. C. - Nuclear Fusion 25, 1101 (1985).

3 - KARGER F., KLÜBER O., *et al* Nuclear Fusion 25, 1059 (1985) G., MC CONCK K., MEISEL D. SESNICK S. - 5th International Conference on Plasma Physics and Controlled Nuclear Fusion Research (Tokyo) Vienna, IAEA, 1, 207 (1974).

4 - VANNUCCI A., BENDER O. W., CALDAS I. L., TAN I. H., NASCIMENTO I. C., SANADA E. K. - Il Nuovo Cimento, 10 D, 1193 (1988).

5 - VANNUCCI A., NASCIMENTO I. C., CALDAS I. L.- Plasma Physics and Controlled Fusion, 31, 147 (1989).

6 - VANNUCCI A., GILL R. D. - Nuclear Fusion 31, 1127 (1991).

7 - LICHTENBERG A. I., LIBERMAN M. A. - Regular and Stochastic Motion, Springer Verlag, New York (1983).

8 - FERNANDES A. S., HELLER M. V. A. P., CALDAS I. L.- Plasma Physics and Controlled Fusion 30, 1203 (1989).

9 - FILONENKO N. N., SAGDEEV R. Z., ZASLAVSKY G. M. - Nuclear Fusion 7, 253 (1967).

10 - KERST D. W., J. Nucl. Energy PtC 4, 253 (1962).

11 - PERCIVAL I., RICHARDS D. - Introduction to Dynamics, chap. 7, Cambridge University Press (1982).

12 - FUSSMAN G., GREEN B. J., ZEHRFELD H. P.- 8th International Conference on Plasma Physics and Controlled Nuclear Fusion Research, 1980 (Brussels) Vienna, IAEA, 1, 353.

13 - RAMOS DE ANDRADE M. C. - M.Sc. Dissertation (in Portuguese), Institute of Physics, University of São Paulo - 1989.

14 - ESCANDE D. F., DOVEIL F. - Journal of Statistical Physics 26, 257 (1981).

15 - HELLER M. A. V. P., CALDAS I. L., ANDRADE M. C. R. - Nonlinear Phenomena in Fluids, Solids and Other Complex Systems, edited by P. Cordero and B. Nachtergaele, Elsevier Science Publishers B. V., 83 (1991).

Fig.1 Coordinate system and outline of the helical windings on the toroidal camera.

Fig.2 Frequency ω as a function of $\rho/(a^2/2)$ obtained from the eqs.(13) (a) and eq.(17) (b), for I = 100A, q(a) = 5, q(0) = 1 and I_p = 10kA.

Fig.3 Poincaré map of the field line trajectories for I_h = 100A, ϵ = 0.27, q(a) = 5, q(0) = 1 and I_p = 10kA.

Fig.4 Map of field line trajectories in the plane J×θ for $u_0 = \pi/2$ (o) (r_0 = 5.8 cm and 6.4 cm) and for u_0 = 0 (o) (r_0 = 5.8cm, 5.5cm and 4.7cm) obtained by integrating eqs.(21) and considering the same parameters of the Fig.3.

Fig.5 Map of field line trajectories in the plane J×θ obtained by integrating the exact field line eqs.(4) and considering the same parameters of the Fig.3.

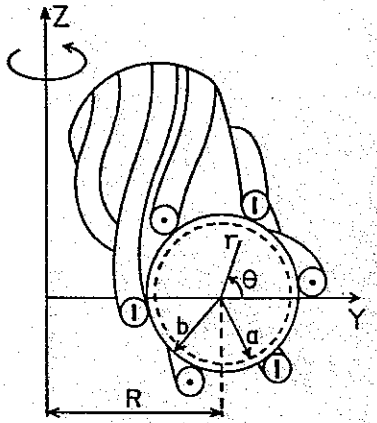

Fig. 1

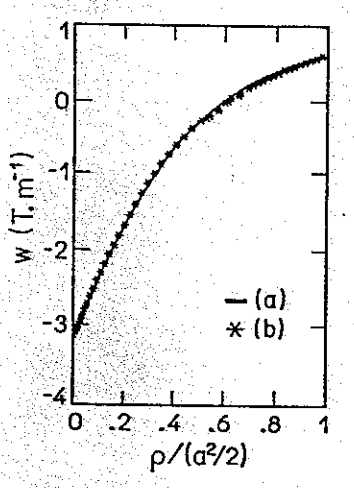

Fig. 2

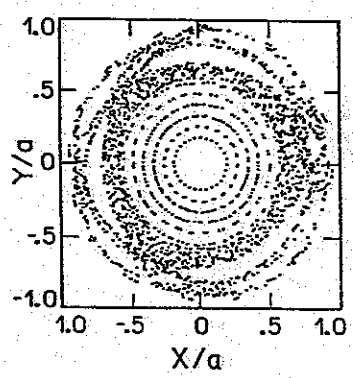

Fig. 3

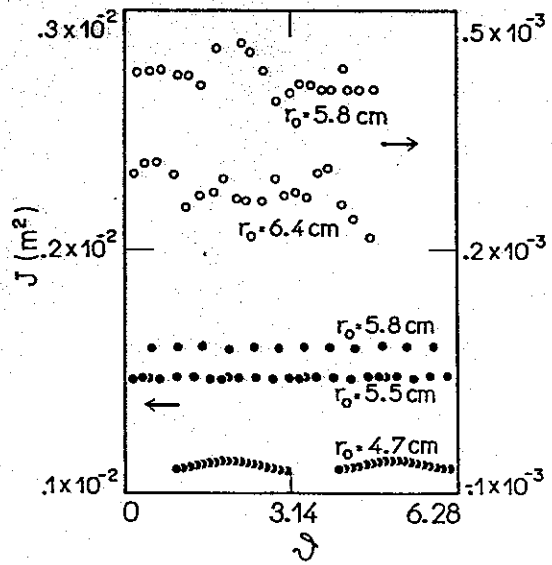

Fig. 4

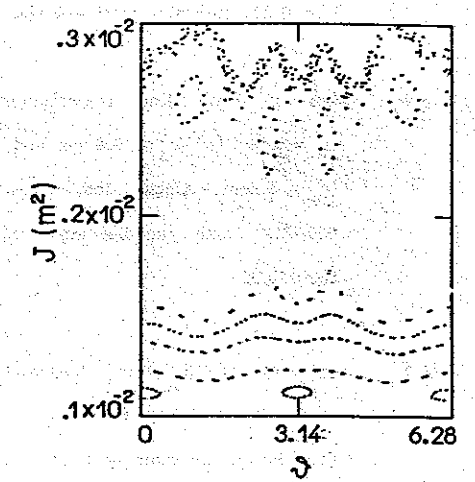

Fig. 5